Ship wake field analysis using a coupled BEMt-RANS approach

Charles Badoe[1*], *Alexander Phillips*[1] and *Stephen R Turnock*[1]

[1] Faculty of Engineering and the Environment, University of Southampton, Southampton, UK
Email: cb3e09@soton.ac.uk

** Corresponding author*

1. Introduction

The prediction of a ship's wake field and self-propulsion capabilities has traditionally been centered on experiments; however with the advancement in modern computing power, this can be achieved through the use of computational methods. An advantage with the use of CFD is its ability to provide insight into flow characteristics close to the wall, which are difficult to obtain through experiments. The most interesting and challenging aspect of using CFD in this analysis, is the influence of the propeller action and the unsteady hydrodynamic of the rudder working in the propeller wake. One approach to address the problem is to discretize the ship, propulsor and the rudder using unsteady RANS computations (Carrica et al., 2011). Due to the small time steps and high computational cost involved, simulations are often performed using representative propeller models or body force method. The level of complexities in the body force propeller approach varies from prescribing the body forces, Badoe et al., (2012), Phillips et al., (2010), through to coupling a more complex propeller performance code which accounts for the non-uniform inflow at the propeller plane, Phillips et al., (2009). There are several self-propulsion computations using body force propeller models reported in the literature. Banks et al., (2010) performed a RANS simulation of multiphase flow around the KCS hull form using a propeller model with force distribution based on the Hough and Ordway thrust and torque distribution (Hough and Ordway, 1965). Simonsen and Stern, (2003) coupled a body force propeller model based on potential theory formulation in which the propeller was represented by bound vortex sheets on the propeller disk and free vortices shed from the downstream of the propeller to a RANS code to simulate the manoeuvring characteristic of the Esso Osaka with a rudder.

In the present work an investigation is carried out into the sensitivity with which the wakefield of a container ship in calm water is resolved using a coupled BEMt-RANS sectorial approach.

2. Theoretical approach

2.1. RANS approach

The flow generated around the BEMt propeller model and hull can be modeled by the unsteady Reynolds averaged Navier-Stokes equations. Within the assumption of an incompressible fluid, the set of equations may be written in the form:-

$$\frac{\partial \overline{U_i}}{\partial x_i} = 0 \qquad [1]$$

$$\frac{\partial \overline{U_i}}{\partial t} + \frac{\partial \overline{U_i}\overline{U_j}}{\partial x_j} = -\frac{1}{\rho}\frac{\partial \overline{P}}{\partial x_i} + \frac{\partial}{\partial x_j}\left\{\nu\left(\frac{\partial \overline{U_i}}{\partial x_j} + \frac{\partial \overline{U_j}}{\partial x_i}\right)\right\} - \frac{\partial \overline{u'_i u'_j}}{\partial x_j} + \overline{f_i} \qquad [2]$$

where x_i represents the Cartesian coordinates (X, Y, Z) and U_i are the Cartesian mean velocity components ($\overline{U_x}$, $\overline{U_y}$, $\overline{U_z}$). The Reynolds stress is expressed as ($\overline{u'_i u'_j}$) and must be modeled using an appropriate turbulence model.

2.2. BEMt propeller model and coupling methodology

BEMt is a method of modelling the performance of tidal turbines, (Mikkelsen, 2003) and ship propellers, (Phillips, 2009). The method combines both the blade element theory and the momentum theory. By combining these two theories, some of the difficulties involved in the calculation of the induced velocity of the propeller are addressed. Solution to this problem can be achieved if the part of the propeller between r and (r+∂r) is analysed by matching forces generated by the blade elements, as 2D lifting foils to the momentum changes occurring through the propeller disc between these radii. An actual propeller is not uniformly loaded as assumed by Rankine and Froude actuator disc model, thus to analyze the radial variation of loads along the blade the flow field is divided into radially independent annulus stream tube.

An existing BEMt code (Molland and Turnock, 1996) was modified and coupled to a RANS solver, whereby within the RANS mesh the propeller is represented as a cylindrical domain with diameter equal to that of the propeller diameter, D and a length of 0.1D. The propeller is adapted to the hull wake by employing a sectorial approach where the propeller domain is sub divided into a series of nC circumferential, and nR radial slices along the blade. An example of a BEMt mesh is presented in Fig. 1. A brief coupling procedure is presented as follows:

1. A steady state RANS computation is first performed with the body force terms set to zero.
2. The resulting local nominal wake fraction is determined for each radius by calculating the average mean circumferential velocity at the corresponding radius. This procedure captures the influence of the rudder and hull on the flow through and across the propeller disc.

$$W_T{}'' = \frac{1}{2\pi r} \int_0^{2\pi} \left(1 - \frac{U}{U_a}\right) r \, \partial\theta \qquad [3]$$

   where U signifies the axial velocity at a given nC circumferential, and nR radial location.
3. The BEMt propeller code iterates to find the local thrust and torque for nR radial and nC circumferential locations based on the local nominal wake fraction, the inflow speed and the rps.
4. The local thrust and torque are assumed to act uniformly over the circumference corresponding to each radial slice. They are then converted into axial and tangential momentum sources and distributed over the nR radial and nC circumferential slices respectively.
5. The Simulation is then started from the naked hull and rudder solutions but now with the added momentum sources until convergence is achieved.
6. The effective wakefield is defined by repeating steps 2 to 5 to find the total wakefield then subtracting the propeller induced velocities calculated from the BEMt code.

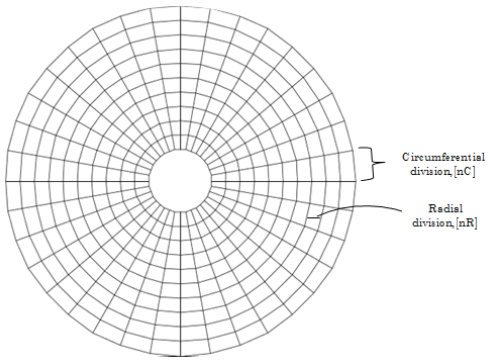

Fig. 1: BEMt propeller mesh showing radial, nR, and circumferential, nC, subdivisions

3. Ship model wake field analysis case study

3.1. Details of experiment

The case considered is the self-propelled KRISO container ship (see Fig. 2 and Table 1) in calm water conditions (Larsson et al., 2010). The MOERI scale KCS hull model, designed at KRISO and tested at SRI, (Fujisawa et al., (2000) was used for this study. Measurements of local velocity field on the MOERI KCS hull was carried out at SRI's towing tank (400m long x 18m breadth x 8m depth) at Froude number Fn=0.26 under even keel conditions. The rate of the propeller model was set at 9.5rps and self-propulsion condition at "ship point". Full details of the experimental conditions and data can be found at Fujisawa et al., (2000).

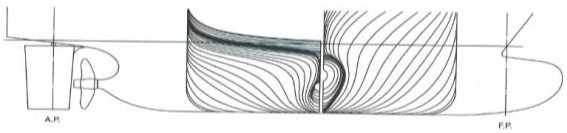

Fig. 2. Body plan and side profile of the KCS ship model, source: Fujisawa et al., (2000).

3. Simulation setup

Numerical solution of equations (1) and (2) was carried out using the open source RANS solver OpenFOAM, which is designed to solve problems in mechanics of continuous mediums; see Jasak (1996)

for more details on introduction and numeric used in OpenFOAM. The steady RANS equations were solved using a cell centered finite volume method (FVM). Discretization of the convection terms was achieved using Gauss linear second order upwind and the diffusion terms were treated using the central difference scheme. The SIMPLE algorithm was used for the pressure-velocity coupling. The pressure correction equation was under relaxed with a factor of 0.3, which was found as a compromise between stability and convergence speed.

The SST k-ω model has been successfully used for this purpose of hull-propeller-rudder interaction and wakefield analysis, (Larsson et al., 2010) making it a natural choice for the study discussed herein.

Table 1: Principal dimensions of the KCS model and propeller.

Dimensions	Full scale	Model scale MOERI
Scale	1.00	31.5994
L_{PP} (m)	230.0	7.2785
B_{WL} (m)	32.2	1.0190
D (m)	19.0	0.5696
T (m)	10.8	0.3418
Displacement (m^3)	52030	1.6497
Rudder type	SB horn rudder	-
Lat. area (m^2)	54.45	-
Propeller type	FP	FP
Number of blades, N	5	5
Diameter (m)	7.9	0.250
P/D at 0.7R	0.997	0.9967
Ae/Ao	0.800	0800
Rotation	Right	Right
Hub ratio	0.180	0.1800

4.1. Boundary Conditions

The inflow and outflow plane were located 1.2LPP in front of and 2.5LPP behind the hull respectively. The hull, rudder and propeller were modelled as no-slip walls, the sides and bottom of the domain were treated using slip boundary condition. The influence of free surface was not included in the simulation due to the increase cost in computation hence the free surface was modelled with a symmetry plane.

4.2. Grid generation

Unstructured, predominantly hexahedral grids with local refinements around no slip walls were used in the study. All grids were created using blockMesh and snappyHexMesh utilities forming part of the OpenFOAM libraries. The grids were congregated in the regions of the stern, bow, near the hull surface and the free surface. Ten to twelve elements were used to capture the boundary layer of the hull and rudder yielding an approximate y^+ of 60 for the hull and 30 for the rudder. The total number of grids used was approximately 5 million. Fig. 3 shows the mesh resolution for the bow and stern.

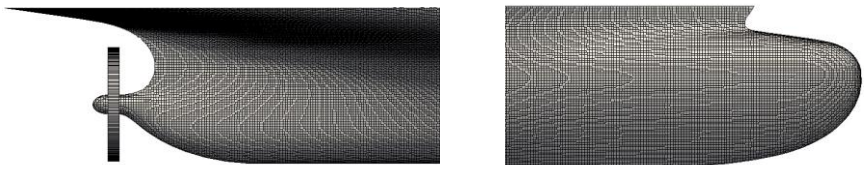

Fig. 3. KCS bow and stern mesh.

5. Results

5.1 Propeller Open water prediction

The open water performance shown in Fig. 4 calculated from the BEMt propeller code is compared with values from SRI. The trend in KT plots highlights the good agreement of the predicted thrust of the propeller. The BEMt model showed an over prediction in torque ($10K_Q$), and the discrepancies increased as the propeller advance coefficient (J) reduces. This

is not unusual especially when using momentum theory in the numerical prediction of propeller open water conditions. This has also been reported by Uto, (1993) who carried out RANS simulations involving marine propellers. These over predictions might be unavoidable due to experimental conditions such as tunnel wall, inflow speed non-uniformity and hub and boss configurations which do not conform to CFD simulations. For the effective advance speed of interest for this work (nominal J=0.7) the agreement for KT and 10 KQ was excellent with difference of less than 4%.

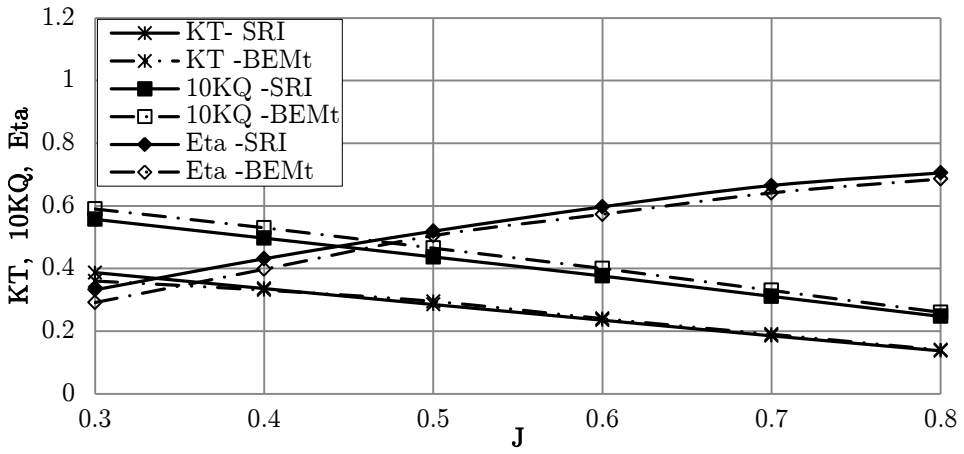

Fig. 4. Comparison of propeller characteristics in open water. Experiments data Fujisawa et al., (2000).

5.2 Nominal wakefield predictions

The prediction of a ships nominal wakefield is important since it provides a good initial estimate for the BEMt-RANS propeller model. The local velocity field without the working propeller model at an even keel 0.25D behind the propeller plane is compared with that of SRI in Fig. 5. The symmetry with respect to the ships centreline is well predicted compared to experiments up to u ≈0.7. The diffusive contour lines of u ≈0.8&0.9 at the top part of the propeller outer radius (both port and starboard) are likely the result of insufficient mesh resolution around that region. The distortion in the velocity, i.e. the "hook shape" is very small compared to that of the experiment. Other distinct flow features such as the weak vortex flow found on both sides near the upper corner of the propeller boss and the downwards flow found near the centreline above the shaft were accurately predicted. The averaged nominal wake 1-wn was 1% over estimated at 0.720 compared to SRI's value of 0.712.

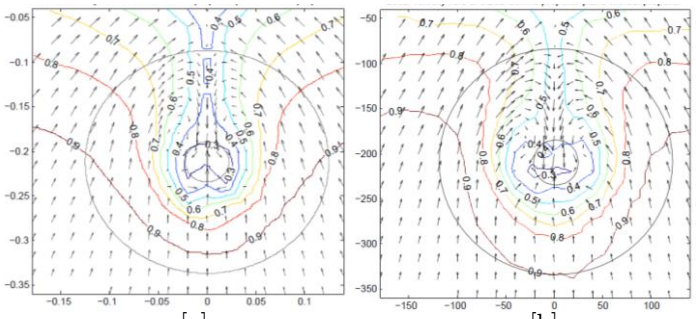

[a] [b]

Fig. 5: Local velocity field (u contour & v-w vectors) 0.25D behind propeller plane (x/L=0.491), Fr 0.26 without propeller [a] Fine grid, [b] Experiment, SRI.

5.3 Sensitivity studies

Sensitivity studies were carried on the BEMt model to determine the number of radial nR, and circumferential, nC, subdivisions to effectively capture the wake field with the working propeller. A series of radial subdivisions, nR =10, 20, 40 and circumferential, nC subdivisions from 10-360 were used. It can be seen from the convergence plot in Fig. 6 that nC converges at about 100 subdivisions. The plots in Fig. 7 were then created by fixing nC to 180 and the varying nR. The plots were taken with the working propeller. It can be seen from the plots that when nR > 20 the wake is smeared out. Not enough thrust is generated by the BEMt beyond this point. The reason for this behaviour may is yet to be established, nevertheless the wake field is predicted reasonably well by using nR=20 and nC =180

(Fig. 7b). By comparing Fig. 7b to that of a BEMt model which assumes an average wakefield as in Fig. 7d, the superiority of the sectorial approach is clearly illustrated. The sectorial approach is seen to be more consistent with a real propeller hydrodynamic influence on the inflow (Fig. 7e). The approach does not use an average circumferential distribution but rather takes into account the local thrust and torque at each radial and circumferential location in the propeller plane. This results in an asymmetry in the flow field.

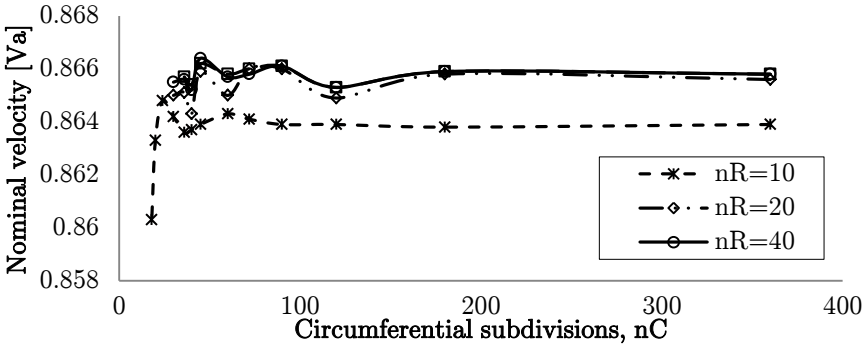

Fig.6 : Convergence of nominal velocities for various radial, nR, and circumferential, nC, subdivisions.

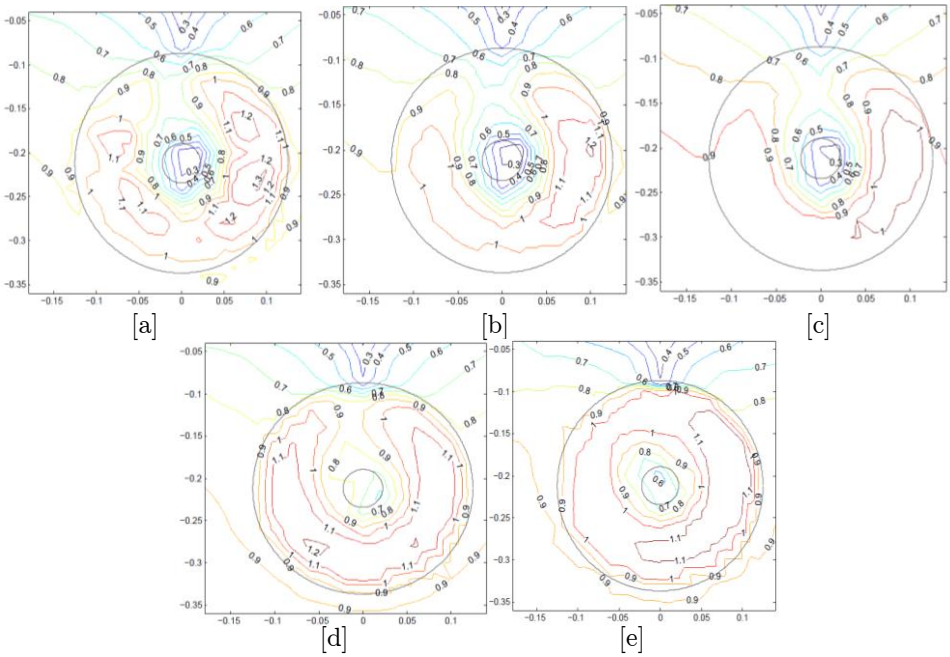

Fig. 7: BEMt sensitivity studies for local velocity field (u contour) 0.25D behind propeller plane (x/L=0.491), Fr 0.26 with [a] nR =10 [b] nR =20 [c] nR =40 [d] Averaged wake [e] Experiment, SRI, at n_p = 9.5rps.

5.3 Self-propulsion parameters

The self-propulsion parameters shown in Table 2 also compares well with the experiment. It should however be borne in mind that propeller forces are dependent on the inflow conditions (bare hull wake) hence a slight over-prediction in the hull wake will result in an increased inflow velocity to the propeller, causing an increase in propeller forces hence the over-prediction in the thrust and torque values.

Table 2: Self-propulsion parameters for KCS in fixed condition.

Parameter	BEMt	SRI	*E*%D
K_T	0.1830	0.1703	+7%
K_Q	0.0315	0.0288	+9%

NB: Tabulated results obtained using nR =20& nC =180 as shown in Fig. 6b.

6. Conclusions

An inviscid-viscous coupling methodology has been outlined to analyse the wakefied of a containership in calm water conditions. These initial results have indicated that the sectorial approach described has much merit for capturing many aspects of wakefield of ships in calm water conditions. The wakefield was poorly predicted when nR>20. The reason for this behaviour is yet to be established but one possible reason might be due to the mapping of data from the BEMt to the RANS mesh. There is still much scope for detailed analysis of the sectorial approach and the empirical relations used in the BEMt code.

References

Badoe, C., Phillips, A.B. and Turnock, S.R., (2012), Initial numerical propeller rudder interaction studies to assist fuel efficient shipping, in 'Proceedings of the 15th Numerical Towing Tank Symposium, 7-9 October, Cortona Italy'.

Banks, J., Phillips, A.B., Turnock, S.R. and Bull, P.W., 2010. RANS simulations of multiphase flow around the KCS hull form. In, *Gothenburg 2010*, *A workshop on CFD in ship hydrodynamics* 08-10 December.

Carrica, P.M., Alejandro, M., and Stern, F., 2011. Full scale self-propulsion computations using a discretized propeller for the KRISO container ship KCS. Journal of computers and fluids marine science and technology, 51, pp.35-47.

Fujisawa, J., Ukon, Y., Kume, K., and Takeshi, H., 2000, Local Velocity Measurements Around the KCS Model (SRI M.S. No. 631) in the SRI 400m Towing Tank, Ship Perf. Div. Rep. No. 00-003-2, SRI, Tokyo, Japan.

Goldstein, S., 1929. On the Vortex Theory of Screw Propellers. Proc. of the Royal Society, 123, 440, (A).

Hino, T., 2005. CFD workshop Tokyo. In Proceedings of the CFD Workshop Tokyo, National Maritime Institute of Japan.

Hough, G.R. and Ordway, D.E., 1965. The generalized actuator disc. Developments in theoretical and applied mechanics, 2, 317-336.

Jasak, H., 1996. Error analysis and estimation for the finite volume method with applications to fluid flows, Ph.D thesis, Imperial College of Science, Technology and Medicine, University of London.

Larsson, L., Stern, F., and Bertram, V., 2003. Benchmarking of Computational Fluid Dynamics for Ship Flows: The Gothenburg 2000 Workshop. Journal Ship Research, 47, pp.63–81.

Larsson, L., and Zou, L., 2010. CFD prediction of local flow around the KVLCC2 tanker in fixed condition. A Workshop on Numerical Ship Hydrodynamics: The Gothenburg 2010 Workshop December 8-10, 2010.

Menter, F.R., 1994. Two-equation eddy viscosity turbulence models for engineering applications. AIAA journal, 32(8), pp.1598–605.

Mikkelsen, R., 2003. *Actuator Disc Methods Applied to Wind Turbines*, Ph.D thesis, University of Denmark.

Molland, A.F., and Turnock, S.R., 1996. A compact computational method for predicting forces on a rudder in a propeller slipstream. Transactions of the Royal Institution of Naval Architects, 138, pp.227–244.

Phillips, A.B., Turnock, S.R. and Furlong, M.E., 2009. Evaluation of manoeuvring coefficients of a self-propelled ship using a blade element momentum propeller model coupled to a Reynolds averaged Navier-Stokes flow solver. *Journal of ocean engineering*, 36(15-16), pp.1217-1225.

Phillips, A.B., Turnock, S.R. and Furlong, M.E., 2010. Accurate capture of rudder-propeller interaction using a coupled blade element momentum-RANS approach. *Journal of Ship Technology Research*, 57(2), pp.128–139.

Simonsen, C., and Stern, F., 2003. Verification and Validation of RANS manoeuvring simulation of Esso Osaka: effects of drift and rudder angle on forces and moments. Journal of Computers and Fluids, 32, pp.1325-1356.

Stern, F., Agdrup, K., (Eds.)., 2008. SIMMAN 2008, Workshop on verification and validation of ship maneuvering simulation methods. In Draft workshop proceedings.

Uto, S. (1993), 'Computation of incompressible flow around a marine propeller', Journal of Naval Architecture 173.